

Plasmonic laser antenna

Ertugrul Cubukcu, Eric A. Kort, Kenneth B. Crozier,^{a),b)} and Federico Capasso^{a),c)}
*Division of Engineering and Applied Sciences, Harvard University, 29 Oxford St., Cambridge,
 Massachusetts 02138*

(Received 22 June 2006; accepted 26 July 2006; published online 31 August 2006)

The authors have demonstrated a surface plasmon device composed of a resonant optical antenna integrated on the facet of a commercial diode laser, termed a plasmonic laser antenna. This device generates enhanced and spatially confined optical near fields. Spot sizes of a few tens of nanometers have been measured at a wavelength $\sim 0.8 \mu\text{m}$. This device can be implemented in a wide variety of semiconductor lasers emitting in spectral regions ranging from the visible to the far infrared, including quantum cascade lasers. It is potentially useful in many applications including near-field optical microscopes, optical data storage, and heat-assisted magnetic recording. © 2006 American Institute of Physics. [DOI: 10.1063/1.2339286]

Surface plasmons (SPs) are collective excitations of the electron plasma in a metal by electromagnetic radiation.^{1,2} They have been extensively used in various applications ranging from biosensors to near-field optical microscopes and devices. Early applications such as SP microscopy,³ some of which have achieved single atomic layer sensitivity,⁴ and surface enhanced Raman spectroscopy⁵ made use of plasmon excitation in thin metals.

Optical antennas are single or coupled metallic nanoparticles in which optical excitation of surface plasmons can produce very high intensities in the optical near field. The field enhancement relative to the incident field is maximum when the wavelength is suitably matched to the size of the resonant nanoparticle. Optical antennas were first demonstrated at microwave frequencies⁶ and more recently at mid-infrared⁷ and near-infrared^{8–10} frequencies. Of particular interest are resonant optical antennas comprised of a pair of strongly coupled metallic nanorods. This design leads to a large intensity enhancement localized in the gap between the latter.⁹

The enhanced transmission of light through subwavelength apertures and aperture arrays in metal films, a phenomenon associated with SPs, has also attracted considerable interest.¹¹ Very small aperture lasers that consist of a laser diode with its facet coated by a metal film on which a subwavelength aperture is etched by FIB milling have been demonstrated.^{12,13} However, these devices suffer from limited output power even though the transmission is enhanced when normalized to the aperture area.

In this work, we propose and demonstrate a photonic device, the plasmonic laser antenna, which consists of a resonant optical antenna integrated on the facet of a laser diode. Such a compact laser source with subwavelength spatial resolution provides distinct advantages in a number of applications including microscopy, spectroscopy, optical data storage, lithography, and laser processing.

A schematic of the proposed device is shown in Fig. 1. A pair of coupled triangle-like particles (for example, a bow tie antenna)^{6,8} or of nanorods⁹ separated by a very small gap, which is less than 30 nm in this work, is defined on one of

the facets of a diode laser. Gold nanorods can generate enhanced near fields through the excitation of SPs.¹⁴ The large field enhancement in these structures, compared to gold nanospheres, is due to the substantially reduced plasmon dephasing rate, an effect caused by suppression of interband damping at near-infrared wavelengths.¹⁵

Aizpurua *et al.*¹⁶ carried out a numerical study of field enhancement with single and coupled nanorods. This work showed that in the latter a strongly localized intense optical spot in the nanoscale gap between the rods can be generated. This is due to capacitive coupling as the charges on the nanorod ends that define the gap have opposite signs. Hence, the enhanced field in the gap is mostly polarized along the length of the antenna. In the plasmonic device that we propose here, the size of the intense optical spot is largely determined by the size of the gap; a major advantage is that this scheme does not suffer from limited throughput as no subwavelength apertures are involved. With an aperture, the size of the optical spot can be equally small, but the power that can transmit through such a small subwavelength aperture will decay as the fourth power of the aperture diameter when the latter is smaller than one-quarter of the illumination wavelength.¹⁷

We modeled optical antennas on alumina substrate by using a finite difference time domain code (FULLWAVE, Rsoft-design Inc.). The structures consist of two coupled gold nanorods separated by a 20 nm gap. This allowed us to determine the resonant antenna lengths for an excitation

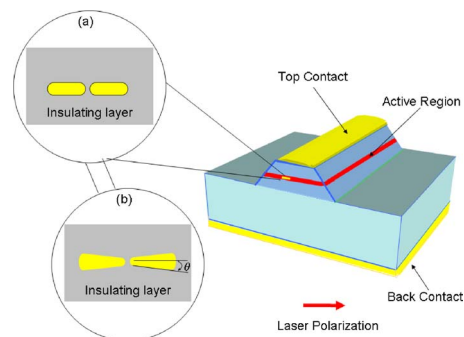


FIG. 1. (Color online) Plasmonic laser antenna: (a) nanorod design employed in this work and (b) bow tie design that would provide a stronger contrast between the intensity enhancement in the gap and the intensity enhancement at the ends of the antenna.

^{a)} Authors to whom correspondence should be addressed.

^{b)} Electronic mail: kcrozier@deas.harvard.edu

^{c)} Electronic mail: capasso@deas.harvard.edu

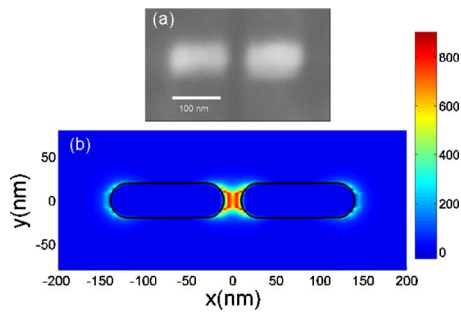


FIG. 2. (Color online) (a) Scanning electron micrograph of the resonant optical antenna. (b) Numerical simulation of the total electric field intensity enhancement with respect to the incident intensity. The enhancement reaches values ~ 800 near the middle of the gap.

wavelength of 830 nm. Physically resonance is achieved when the length of each nanorod approximately equals an odd integer number of half SP wavelengths.⁷ The width and thickness of the nanorods are both 50 nm. The ends of the nanorods are rounded off, with a radius of curvature of 25 nm, similar to the fabricated structures. We used $0.188 + 5.39i$ for the complex refractive index of gold.¹⁸ Our simulations indicate that the first resonant length is ≈ 130 nm and the second one is ≈ 550 nm. The electric field intensity enhancements in the gap normalized to the incident intensity are ≈ 800 and ≈ 400 for the first and second resonances, respectively. These resonances are referred to as the first two dipole active modes,¹⁶ or as $\lambda/2$ and $3\lambda/2$ antennas in antenna theory.¹⁹

For the first resonance, the steady-state time-averaged total electric field intensity distribution around the optical antenna is shown in Fig. 2(b). Here the incident plane wave illumination is polarized along the antenna axis. We fabricated an optical antenna structure on a commercial edge-emitting laser diode (made by Sanyo Inc.) operating at a wavelength of 830 nm, which incorporates a photodiode to monitor the power from the back facet. To prevent electrical shorting of the laser and the monitor photodiode in the laser package, Al_2O_3 (~ 280 nm thick) was deposited first onto the laser facet as an insulating layer. A gold layer was then evaporated onto the Al_2O_3 film. Next the optical antenna in Fig. 2(a) was defined by FIB milling. It consists of two gold nanorods separated by a gap of ≈ 30 nm. Each nanorod is ≈ 130 nm long, ≈ 50 nm wide, and ≈ 50 nm thick.

We performed scanning near-field optical microscopy to measure the optical near-field distribution in the fabricated devices. It has been shown that apertureless near-field scanning optical microscopy (*a*-NSOM) can be used to study the optical near field of an aperture fabricated on a laser diode.¹³ We employed an *a*-NSOM in a similar manner.¹³ In this technique, light is scattered by the end of a sharp atomic force microscope (AFM) tip.^{20–22} The AFM cantilever is driven at its resonant oscillation frequency, and the light scattered by the tip is collected by the back-facet photodiode. Lock-in detection is used to extract the component of the scattered light at the cantilever oscillation frequency. The resulting signal gives an image of the optical near-field intensity. While the tip is in close proximity to the antenna gap, the evanescent fields excite SPs in the tip, which in turn radiates a signal detected by the photodiode. The gold-coated AFM tip can be modeled as a dipole interacting with its image in the underlying material.²¹ The near-field imaging technique used here is sensitive to the light polarized along

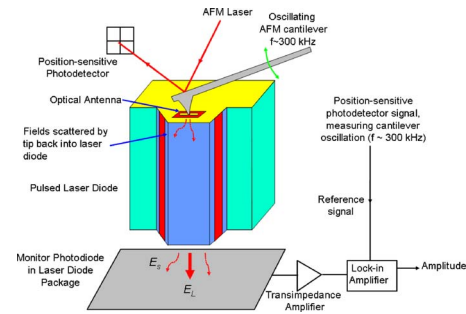


FIG. 3. (Color online) Experimental setup for measurement of near-field intensity distributions on plasmonic laser antennas. The instrument is a conventional *a*-NSOM/AFM operated in noncontact mode. Topographic and optical near-field images are obtained simultaneously. The optical near-field image is obtained by monitoring the power output from the photodiode. Lock-in detection at the cantilever oscillation frequency is used to extract the component of the photodiode signal resulting from scattering by the AFM tip, which constitutes the optical near-field image.

the height of the pyramidal AFM tip. In conventional AFMs the cantilever is mounted at a tilt and therefore scatters out a combination of all x , y , and z components of the electric field with weights that are difficult to determine. This makes a direct comparison between the simulations and the experiments difficult.

Our experimental setup is shown in Fig. 3. The laser diode is driven by a pulsed current source since continuous wave (cw) operation caused the antennas to melt. Unaltered lasers can emit up to 30 mW of power in cw mode, which is well above the damage threshold of gold. To minimize heating effects the laser was operated at a low duty cycle with a pulse length of 20 ns and a repetition frequency of 2 MHz. In particular, the near-field optical images shown in Fig. 4 were obtained with the diode laser biased so that the average optical power measured with a large area photodiode in the far field was 0.3 mW at 4% duty cycle, corresponding to a peak power of 7.5 mW. The plasmonic laser antenna device was mounted in a conventional atomic force microscope (PSIA XE-120). A metallized AFM tip is then used in non-contact mode with the surface, where it is modulated at ~ 300 kHz while the sample is scanned underneath it. While mapping out the topography in this typical AFM manner, we also measure the optical near-field intensity distribution. Light is scattered by the metallized AFM tip; while this radiation reaches the monitor photodiode predominantly back through the laser diode, a fraction of it is also collected by repeated scattering off the cantilever.¹³ The signal from the photodiode is then amplified and fed into a lock-in amplifier where a phase sensitive measurement is performed using as a reference the frequency of the AFM cantilever.

Figure 4 shows the results of our measurements. The full width at half maximum of the central peak of the near-field intensity distribution is 40 nm in the x direction and 100 nm in the y direction [Figs. 4(b) and 4(c)]. This intense optical spot is localized within an area that is 50 times smaller than what one would obtain with conventional optics such as lenses (Rayleigh limit) in addition to the large intensity enhancement, as calculated from our simulations. Such resonant enhancements in the gap are possible only if the incident light is polarized along the antenna structures, hence the antennas are oriented parallel to the active layers of our diode laser, since its emission is TE polarized. We also tested antenna structures with the same parameters, but rotated by 90° , that is, with the incident light polarized perpendicular to

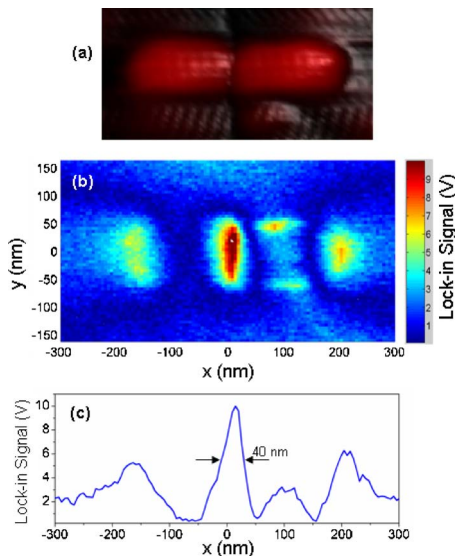


FIG. 4. (Color online) (a) AFM topography and (b) *a*-NSOM image of resonant optical antenna fabricated on one of the facets of a commercial diode laser operating at $\sim 0.83 \mu\text{m}$ wavelength. (c) Line scan of the near-field distribution along the antenna axis

the antenna axis. No intensity enhancement was observed in the gap in these structures.

The fabricated antenna exhibits also field enhancement on the far ends of the nanorods [Figs. 4(b) and 4(c)] as predicted by our simulations. For some applications such as optical data storage where a single optical spot is desired, these multiple spatial peaks around the structure could be problematic. This can be overcome by employing a bow tie design [Fig. 1(b)] since the tapering in the latter produces a “lighting rod” effect so that the fields will be mostly confined in the gap region.^{7,23,24} The small bump seen in the AFM image of Fig. 4(a), below the right-hand side nanorod, is most likely due to nanomasking during FIB patterning, which causes stray near fields in Figs. 4(b) and 4(c). It is likely that the composition of this bump has changed due to doping by Ga ions used in our FIB system and this may be the reason why the near field is perturbed strongly as if this bump acts like a metallic nanoparticle. Since we can only measure the *relative* near-field intensity but not its magnitude, we can only provide an estimate of the actual near-field intensity. Based on the simulated intensity enhancement of 800, an average optical power of 0.3 mW, as used in the experiments of Fig. 4, leads to a peak intensity $\approx 1 \text{ GW/cm}^2$ in the gap. This corresponds to an electric field of 10^5 V/cm at 10 nm above the surface, where the total intensity drops to 20% of its value right on the antenna surface. Such large localized optical intensities are very important for single molecule SERS.

An interesting question is the role that the antenna can have on the operation of the laser. The area of the antenna is less than one-tenth of the estimated size of the mode on the laser facet and the optical antenna radiates in all directions. Thus backreflection from the antenna into the laser is greatly reduced and does not significantly affect its operation. Indeed, no instabilities were detected in the measured optical power.

In summary, we have demonstrated an SP device, the plasmonic laser antenna, which generates intense and highly confined optical fields. We want to stress that resonant optical antennas can be defined on semiconductor lasers emitting in the visible, near-, mid-, and far-infrared spectra, thus including both diode lasers and quantum cascade lasers. We expect that plasmonic laser antennas will be useful in a broad range of applications including optical data storage²⁵ at densities exceeding 1 Tb/in.^2 , orders of magnitude higher than the current highest density digital versatile disks, near-field optical microscopy and spectroscopy, heat-assisted magnetic recording,²³ nanoscale optical lithography,²⁴ as well as spatially resolved chemical imaging and spectroscopy.

Two of the authors (E.C. and F.C.) are supported by the AFOSR under a MURI program. The authors acknowledge support by the NSF NSEC at Harvard University and the Center for Nanoscale Systems (CNS) at Harvard University which is a member of the NNIN.

¹S. A. Maier and H. Atwater, *J. Appl. Phys.* **98**, 1 (2005).

²A. V. Zayats, I. I. Smolyaninov, and A. A. Maradudin, *Phys. Rep.* **408**, 131 (2005).

³B. Rothenhausler and W. Knoll, *Nature (London)* **332**, 615 (1988).

⁴A. N. Grigorenko, P. I. Nikitin, and A. V. Kabashin, *Appl. Phys. Lett.* **75**, 3917 (1999).

⁵S. Nie and S. R. Emory, *Science* **275**, 1102 (1997).

⁶R. D. Grober, R. J. Schoelkopf, and D. E. Prober, *Appl. Phys. Lett.* **70**, 1354 (1997).

⁷K. B. Crozier, A. Sundaramurthy, G. S. Kino, and C. F. Quate, *J. Appl. Phys.* **94**, 4632 (2003).

⁸P. J. Schuck, D. P. Fromm, A. Sundaramurthy, G. S. Kino, and W. E. Moerner, *Phys. Rev. Lett.* **94**, 017402 (2005).

⁹P. Muhschlegel, H. J. Eisler, O. J. F. Martin, B. Hecht, and D. W. Pohl, *Science* **308**, 1607 (2005).

¹⁰J. N. Farahani, D. W. Pohl, H. J. Eisler, and B. Hecht, *Phys. Rev. Lett.* **95**, 017402 (2005).

¹¹T. W. Ebbesen, H. J. Lezec, H. F. Ghaemi, T. Thio, and P. A. Wolff, *Nature (London)* **391**, 667 (1998).

¹²A. Partovi, D. Peale, M. Wuttig, C. A. Murray, G. Zydzik, L. Hopkins, K. Baldwin, W. S. Hobson, J. Wynn, J. Lopata, L. Dhar, R. Chichester, and J. H. Yeh, *Appl. Phys. Lett.* **75**, 1515 (1999).

¹³F. Chen, A. Itagi, J. A. Bain, D. D. Stancil, T. E. Schlesinger, L. Stebounova, G. C. Walker, and B. B. Akhremichev, *Appl. Phys. Lett.* **83**, 3245 (2003).

¹⁴A. Bouhelier, R. Bachelot, G. Lerondel, S. Kostcheev, P. Royer, and G. P. Wiederrecht, *Phys. Rev. Lett.* **95**, 267405 (2005).

¹⁵C. Sönnichsen, T. Franzl, T. Wilk, G. von Plessen, J. Feldmann, O. Wilson, and P. Mulvaney, *Phys. Rev. Lett.* **88**, 077402 (2002).

¹⁶J. Aizpurua, Garnett W. Bryant, L. J. Richter, F. J. Garcia de Abajo, B. K. Kelley, and T. Mallouk, *Phys. Rev. B* **71**, 235420 (2005).

¹⁷X. Shi and L. Hesselink, *Jpn. J. Appl. Phys., Part 1* **41**, 1632 (2002).

¹⁸E. Palik, *Handbook of Optical Constants of Solids* (Academic, New York, 1985), Vol. 1, p. 294.

¹⁹C. A. Balanis, *Antenna Theory, Analysis and Design*, 3rd ed. (Wiley, Hoboken, 2005), pp. 182-184.

²⁰F. Zenhausern, Y. Martin, and H. K. Wickramasinghe, *Science* **269**, 1083, (1995).

²¹B. Knoll and F. Keilmann, *Opt. Commun.* **182**, 321 (2000).

²²B. Knoll and F. Keilmann, *Nature (London)* **399**, 134 (1999).

²³T. Matsumoto, Y. Anzai, T. Shintani, K. Nakamura, and T. Nishida, *Opt. Lett.* **31**, 259 (2006).

²⁴A. Sundaramurthy, P. J. Schuck, N. R. Conley, D. P. Fromm, G. S. Kino, and W. E. Moerner, *Nano Lett.* **6**, 355 (2006).

²⁵P. Herget, T. Ohno, J. A. Bain, K. Takatani, M. Taneya, W. C. Messner, and T. E. Schlesinger, *Jpn. J. Appl. Phys., Part 1* **45**, 1193 (2006).